

Raman micro-spectroscopic map of plastic strain in indented amorphous silica

A. Perriot,¹ V. Martinez,² Ch. Martinet,² B. Champagnon,² D. Vandembroucq,¹ and E. Barthel¹

¹*Surface du Verre et Interfaces,
Unité Mixte de Recherche CNRS/Saint-Gobain,
39, Quai Lucien Lefranc,
93303 Aubervilliers Cedex, France.*

²*Laboratoire de Physico-Chimie des Matériaux Luminescents,
UMR 5620 CNRS/Université Claude Bernard Lyon I,
Domaine scientifique de la Doua, Bât Gabriel Lippmann,
12, rue A.M. Ampère 69622 Villeurbanne Cedex.*

(Dated: May 23, 2019)

Glassy materials are known to exhibit a plastic behavior, in particular in confined geometries. In contrast to metals the plasticity of glasses is characterized by a strong coupling between volumetric and shear strain. We use Raman micro-spectroscopy to estimate the residual densification after indentation in amorphous silica. Using a specific experimental design, the micro-metric resolution of this technique is obtained both at the surface and in-depth. Taking advantage of the high sensitivity to density of the defect lines D1 and D2 associated to vibration modes of three and four-membered silica tetrahedra rings, we obtain a spatially resolved three-dimensional map of indentation induced densification. These local experimental data constitute a guide for a more accurate description of the plastic behavior of silica.

PACS numbers: 62.20.Fe, 78.30.-j, 78.30.Ly

I. INTRODUCTION

Brittleness is a well-known and extensively studied property of silicate glasses. Comparatively, their plastic behavior has remained far less explored. Yet, the latter determines the contact mechanics of the glass surface which are of primary interest for many micron-scale applications.

For obvious historical reasons, the standard vision of plasticity is still largely focused on crystalline materials (especially metals), where irreversible strain is triggered by shear stress and accommodated through volume-conserving dislocations motion. Glasses get out this scope for two different reasons. First, because of their amorphous nature there is no direct equivalent to these dislocation-based mechanisms. Second, being out of equilibrium, the density of glasses is significantly lower than the equilibrium value, making them prone to densify. For this reason, they are called “anomalous” materials. Indeed, silicate glasses densify [1] while experiencing a plastic behavior that can be activated even by a purely hydrostatic loading [2]. This densification process is far from being negligible. Fused silica (density 2.2 g.cm^{-3}), the most anomalous silicate glass of industrial interest, is acknowledged to densify up to about 20 % under mechanical stress [3]. Although this anomalous behavior of fused silica has been known for half a century, in-depth investigations were limited by the brittle nature of silica, which restricts the characteristic size of plastic deformation to micrometer scale. Indeed, evidence of the densification process can only be obtained experimentally in confined geometries, such as in a Diamond-Anvil Cell [2] (DAC) or under an indenter [1], which do not allow direct access to local stress/strain data through the common-used

macroscopic techniques.

We show in this letter that such local data of primary importance can be obtained experimentally through Raman micro-spectroscopy, which has recently proved particularly interesting as a method for local material characterization [4, 5]. Through the combination of a specific method to obtain unaltered cross-sections of indentations with Raman micro-spectroscopy mappings, we provide, for the first time, a map of the local density of the indented area of a fused silica sample. This experimental data on the local strain state of the material constitutes a relevant sieve for the validation of a constitutive law for amorphous silica [3, 6, 7, 8]. Our results evidence that the most sophisticated constitutive law for silica is inaccurate[8]. We show that silica exhibits not only a ductile behavior (at the micrometer scale) but also strain-hardening, once again just like plain metals (owing to a very different elementary mechanism though).

II. EXPERIMENTAL PROCEDURE

Our samples were prepared according to the following procedure. Plates of amorphous silica (Saint-Gobain Quartz IDD), of dimension $10 \times 10 \times 0.4 \text{ cm}^3$, were indented with an instrumented micro-indentation device allowing surface visualization. 2-kg-Vickers indents were performed on these plates, on a previously subcritically-grown crack. We thus obtained, on the crack surface, a cross-section view of the densified material area located under the indent. Indentation curves obtained for these on-crack indentations were similar (loading and unloading curves almost superimpose) with that obtained for plain 2 kg Vickers indentations, showing that the presence of a crack did not noticeably affect the indentation

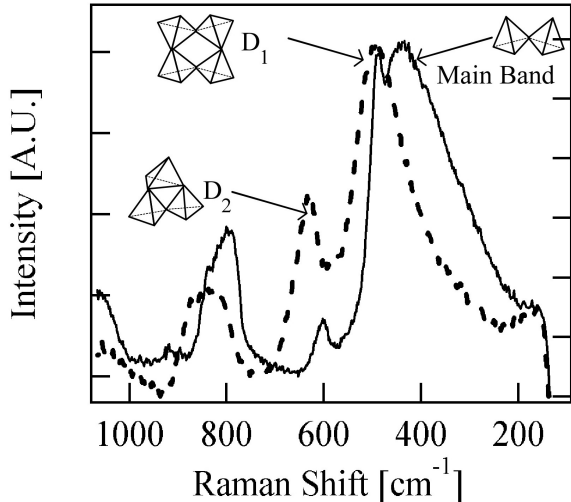


FIG. 1: Raman spectra for amorphous silica. The plain line spectrum was obtained with 2.2 g.cm^{-3} amorphous silica, while the dotted line corresponds to densified amorphous silica.

process. Moreover, the smoothness of the loading curve allows us to describe the indentation process as elasto-plastic.

We used a Raman micro-spectroscopy device (Renishaw RM1000) including a 30 mW 514 nm Argon laser, under a $\times 100$ objective. The laser beam was focused on the surface without confocal system. We evaluated the excited volume of amorphous silica to approximately $2 \times 2 \times 5 \mu\text{m}^3$. After checking densification symmetry with respect to the indenter geometry, we performed surface mappings. We mapped half of the densified area, recording spectra in 42 locations with a $5 \mu\text{m}$ -spacing, according to Fig. 2. We also performed similar measurements on subsurface positions in order to complete the map. For each spectrum, Raman scattering signal was accumulated during 900 s.

III. RESULTS

Between 200 and 750 cm^{-1} , the Raman spectrum of silica glass consists in three bands (Fig. 1 contrasts the Raman spectrum of non-densified fused silica with the spectrum of largely densified silica glass). The main band at 440 cm^{-1} results from the symmetric stretching mode of bridging oxygens between two Si atoms. This band is intense, and affected by the densification process through a decrease of the inter-tetrahedral angles Si-O-Si [9, 10], but it was shown to be also very sensitive to elastic loading [11] (such as the residual elastic strain expected in indentation).

The defect lines D_1 and D_2 , at 492 and 605 cm^{-1} , are respectively attributed to the breathing modes of the four-membered and three-membered rings [12]. The D_2

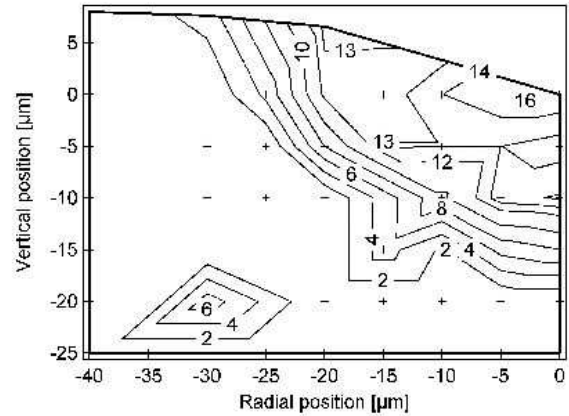


FIG. 2: Densification map of half a section view of an indentation-densified area obtained using the D_2 band position indicator. The center of the indent is at coordinates $(0;0)$. The top bold line represents the sample surface. The dark crosses correspond to the measurement positions. The thin gray lines are the iso-densification lines defined as the lines for which $\Delta\rho/\rho_0$ is constant. Numerical values are given in percent. Iso-densification lines appear to be shaped into concentric bowls. The apparent densification in the bottom-left corner is attributed to an artifact due to a surface contaminant.

line is particularly useful because of its little overlap with the main band. With increasing density, it shifts in position towards higher wavenumbers. Sugiura et al. [13] correlated the position of the D_2 line with the ratio of the sample density ρ to the initial density ρ_0 . From their work, we get the following empirical relation:

$$0.143 \log_{10} \left(\frac{\rho}{\rho_0} \right) = \log_{10} \left(\frac{\nu}{\nu_0} \right) \quad (1)$$

ν and ν_0 being respectively the final and the initial band position. The residual density evaluated through this relation accounts for both irreversible and elastic densification due to residual elastic strain. However, several works [11, 13] evidenced that the D_2 line position is only marginally sensitive to residual elastic strains.

The D_2 peak shift was then used as a density estimator according to equation 1. A typical cross-section map is displayed on Fig. 2. The obtained iso-densification lines are shaped into “concentric bowls”, which agrees with the optical observations by Hagan and Van der Zwaag [14]. Quantitatively, we evaluated the densification just under the indenter tip around 16 %. These results are consistent with the saturation of the densification process that is accepted to occur around 20% [3].

IV. DISCUSSION

A. Yield criterion for amorphous silica

Recently, a hydrostatic-pressure-dependent yield criterion was proposed to describe the plastic behavior of dense amorphous materials like silica glass [3, 6, 7, 8]. Much akin to the Drucker-Prager soil mechanics criterion often used to describe granular materials, this yield criterion is parameterized by two physical characteristics. One of them is the yield strength, Y . The other, known as the densification factor [6] α , balances the respective influence of applied hydrostatic pressure, p , and shear stress, τ , and is analogous to the granular materials friction angle. The plastic yield criterion, $f(\underline{\sigma})$, can thus be written:

$$f(\underline{\sigma}) = \alpha p + (1 - \alpha)\tau - Y \quad (2)$$

The denomination of α as the densification factor appears clearly when one notices that for, $\alpha = 0$, we obtain the Von Mises criterion, which describes the densification-free plasticity of metals, and that, for $\alpha = 1$, we describe a densification-only plastic behavior triggered exclusively by hydrostatic pressure, provided the plastic behavior is associated. The greater α , the more anomalous the material.

Under the assumption of a perfect-plastic and associated behavior, Xin and Lambropoulos [8] attempted to fit those two parameters by comparing experimental load/displacement indentation curve with finite element simulations. With the values $\alpha = 0.6$ and $Y = 5.43$ GPa, they reproduced their experimental data: $\alpha = 0.6$ accounts for a large contribution of densification to plastic strain (even allowing fused silica to exhibit a slight contraction of the cross section while being uniaxially compressed); and the hydrostatic loading yield pressure, obtained for $\tau = 0$, is consistent with DAC experiments [13]. However, indentation experiments result in largely inhomogeneous stress distributions and the mere use of integral data such as indentation curves may prove insufficient to identify the mechanical constitutive law.

B. Densification map as a discriminant sieve

To test the influence of the densification factor on the general shape of the residual densified area, we performed FE calculations, using the FE software Abaqus, to model a cone indentation (of semi-apical angle of 70.2° -making it the “axisymmetric equivalent” to a Vickers indenter). Consistently with Xin and Lambropoulos’ approach [8], the material plastic behavior was assumed perfect and associated until material permanent densification reaches 16%, the value at which saturation occurs and the material cannot densify nor flow any longer. The applied shear strain, τ , was expressed as $J(\underline{\sigma})/\sqrt{3}$, $J(\underline{\sigma})$ being the Von Mises invariant. Calculations were performed

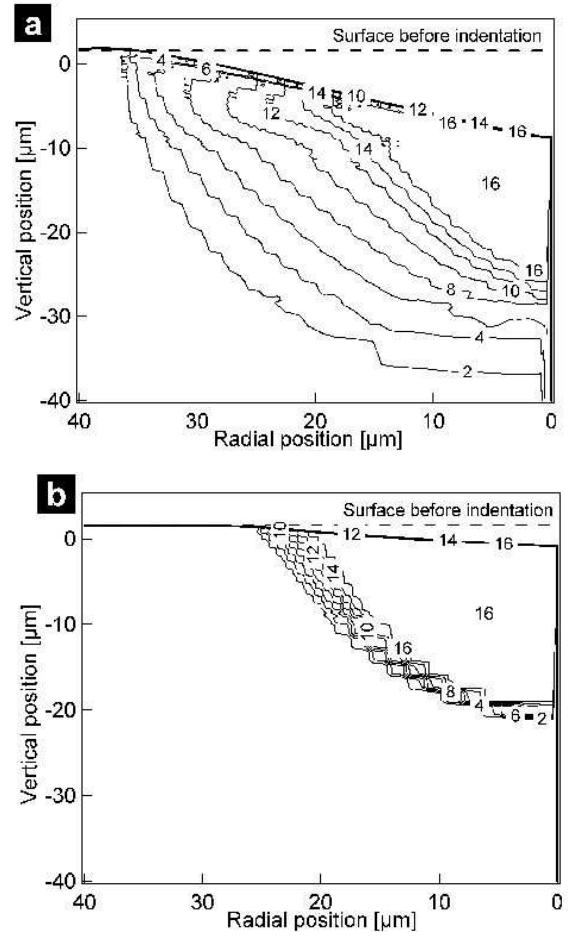


FIG. 3: Residual densification maps obtained through FE simulation of a 2D-axisymmetric cone indentation. They were obtained for two different values of the densification factor, (a) $\alpha = 0.2$ and (b) $\alpha = 0.6$. Densification values are given in percent. The results by Xin and Lambropoulos[8] are similar to (b).

for several values of α ranging between 0.2 and 0.6. The yield strength, Y , was chosen to match the experimental value in hydrostatic conditions ($Y/\alpha = 9.05$ GPa). Residual densification maps for $\alpha = 0.2$ and $\alpha = 0.6$ are presented in Fig. 3. When comparing these two maps, we notice that the indentation-densified areas are markedly different. In the case $\alpha = 0.6$, with a large dependence on hydrostatic contribution, the numerical results predict a small but almost entirely saturated densified area [8]. However, in the less anomalous case $\alpha = 0.2$, the densification area is larger but with a smoother transition towards the non-densified material. This contrast highlights the direct relevance of the density map for the identification of the constitutive law.

C. The role of strain-hardening in amorphous silica plasticity

Let us now compare our experimental density map with the numerical results obtained with the values ($\alpha = 0.6$ and $Y = 5.43$ GPa) proposed in literature [8]. The general shape and extension of the densified area is recovered. This confirms that the densification contribution to the silica plastic behavior is far from being negligible [3, 6, 7, 8]. However, the mainly saturated core with a sharp near-boundary density gradient largely contrasts with the more progressive densification of the experimental result. This shows clearly that indentation curves do not bring enough experimental data to discriminate constitutive laws for silica densification, as they tend to validate constitutive laws that are ruled out by local densification data.

Moreover, it appears that, under the assumption of a hardening-free associated plasticity, none of the parameter sets can reproduce both indentation curves and residual densification maps. At least one of the assumptions made in the constitutive law has to be relaxed. As we expect the material tendency towards densification to progressively decrease with densification taking place, we suggest to account for a silica strain-hardening behavior. We expect this would result in the concentric “bowl-

shaped areas” associated to the experimental smoother density gradient, without much change in the global dimensions of the densified area.

V. CONCLUSION

Raman micro-spectroscopy thus appears to be a very powerful tool to provide accurate and relevant local experimental data for the identification of a constitutive law for amorphous silica. The method could be transposed to other silicate glasses. Moreover, our results clearly suggest that the material densification-hardening has to be accounted for in order to model correctly the “micro-ductile” behavior of silica. On-going work, using Raman micro-spectroscopy coupled with a DAC, currently investigates experimentally silica glass strain-hardening.

VI. ACKNOWLEDGMENTS

The authors would like to thank G. Duisit, R. Gy, S. Pelletier, G. Quérel and S. Roux for their help, advice and support.

[1] E. Taylor, *Nature* **163**, 323 (1949).
[2] H. Sugiura and T. Yamadaya, *J. Non-Cryst. Solids* **144**, 151 (1992).
[3] J. Lambropoulos, S. Xu, and T. Fang, *J. Am. Ceram. Soc.* **79(6)**, 1441 (1996).
[4] A. Kailer, K. Nickel, and Y. Gogotsi, *J. Raman Spectrosc.* **30**, 939 (1999).
[5] S. DiFonzo, W. Jark, S. Lagomarsino, C. Giannini, L. DeCaro, A. Cedolla, and M. Muller, *Nature* **403**, 638 (2000).
[6] M. Imaoka and I. Yasui, *J. Non-Cryst. Solids* **22**, 315 (1976).
[7] A. Shorey, K. Xin, K. Chen, and J. Lambropoulos, *Proc. SPIE* **3424**, 72 (1998).
[8] K. Xin and J. Lambropoulos, *Proc. SPIE* **4102**, 112 (2000).
[9] M. Tomozawa, Y. K. Lee, and Y. L. Peng, *J. Non-Cryst. Solids* **242(2-3)**, 104 (1998).
[10] S. Mochizuki and N. Kawai, *Solid State Communications* **11(6)**, 763 (1972).
[11] T. Michalske, D. Tallant, and W. Smith, *Phys. Chem. Glasses* **29(4)**, 150 (1988).
[12] F. Galeneer, *Solid State Communications* **44(7)**, 1037 (1982).
[13] H. Sugiura, R. Ikeda, K. Kondo, and T. Yamadaya, *J. Appl. Phys.* **81(4)**, 1651 (1997).
[14] J. Hagan and S. V. D. Zwaag, *J. Non-Cryst. Solids* **64**, 249 (1984).